INFERRING THE THERMAL ACCOMMODATION COEFFICIENT FROM TIME-RESOLVED LASER-INDUCED INCANDESCENCE ON IRON NANOPARTICLES

UNIVERSITY OF WATERLOO

T. A. Sipkens[1], W. Richards[1], N. Bizmark[2], N. R. Singh[1], K. J. Daun[1], and M. Ioannidis[2]

[1]Department of Mechanical and Mechatronics Engineering, University of Waterloo

[2]Department of Chemical Engineering, University of Waterloo

MOTIVATION

The unique electromagnetic, chemical, and transport properties of iron nanoparticles have led to many existing and emerging applications [1]:

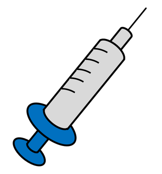

Drug Delivery
They can be used for targeted drug delivery, including improved cancer therapy.

Recording Media
They can be used to improve magnetic-based recording materials, such as hard drives.

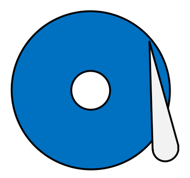

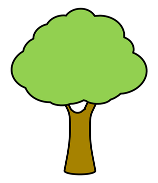

Environment
They are used to catalyze reactions important for environmental remediation.

Medical Imaging
Injecting iron nanoparticles can improve contrast in magnetic resonance imaging (MRI).

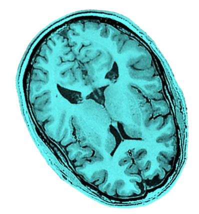

The properties of iron nanoparticles are strongly size-dependant. Accordingly, there is a pressing need for laser-based technologies that can make temporally- and spatially-resolved size measurements of aerosolized iron nanoparticles.

Time-Resolved Laser-Induced Incandescence (TiRe-LII) a combustion diagnostic normally used to size soot primary particles, is being developed as a tool to size iron nanoparticles.

EXPERIMENTAL PROCEDURE

Iron nanoparticles are produced by reducing an aqueous phase ferrous iron solution [2]. The aqueous nanoparticles are then aerosolized using a pneumatic atomizer, and subsequently sized by TiRe-LII.

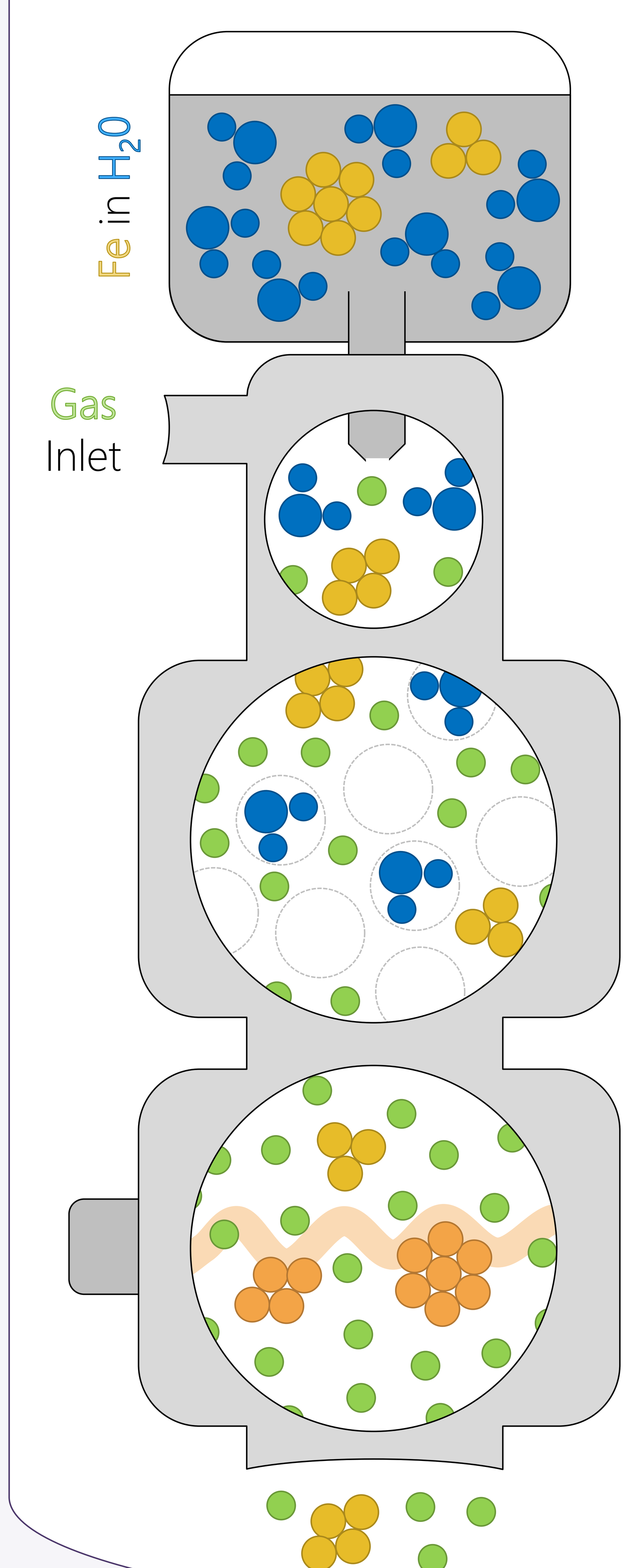

1 Synthesis
A colloidal solution of iron nanoparticles is produced by reacting $FeSO_4 \cdot 7H_2O$ with $NaBH_4$. Dynamic light scattering (DLS) is used to characterize the hydrodynamic size of the nanoparticles. Scanning electron microscopy (SEM) and transmission electron microscopy (TEM) are used to image the nanoparticles.

2 Aerosolize
Iron nanoparticles are aerosolized by flowing a motive gas through a pneumatic atomizer.

3 Drying
The aerosol flows through a diffusion dryer filled with desiccant. The droplets evaporate, leaving the iron nanoparticles behind.

4 TiRe-LII
Time-resolved laser-induced incandescence is used to size the nanoparticles.

TIME-RESOLVED LASER-INDUCED INCANDESCENCE

TiRe-LII involves the following components:

1 Laser Heating
Nanoparticles energized with a 1024 nm Nd:YAG laser pulse.

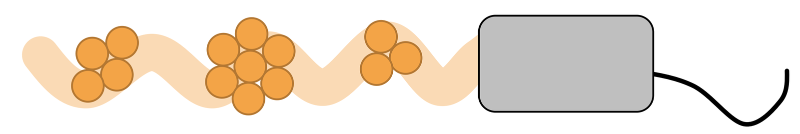

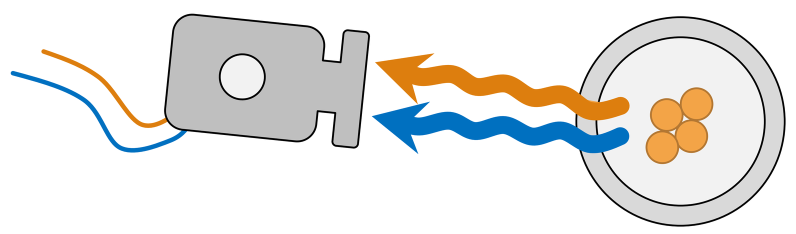

2 Incandescence
Incandescence from the laser-energized nanoparticles is measured at 442 nm and 716 nm.

$$J_\lambda = \int_0^\infty A_c Q_{abs,\lambda}(d_p) P(d_p) E_{b,\lambda}\left[T_p(d_p)\right] d\, d_p$$

3 Heat Transfer Model
Nanoparticle sizes are recovered using a heat transfer model.

$$q_{evap} = \pi d_p^2 m_v N_v'' h_v(T_p)$$

Evaporation
Nanoparticles cool due to vaporization.

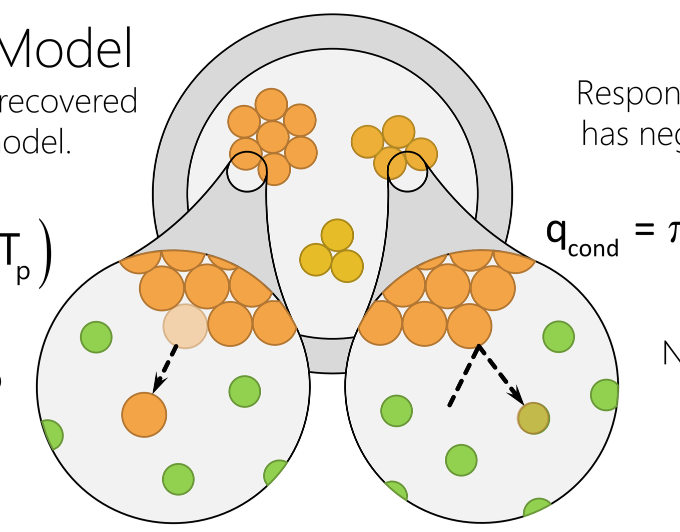

Radiation
Responsible for incandescence, but it has negligible effect on cooling rate.

$$q_{cond} = \pi d_p^2 N_g''(T_g, P_g)\, \alpha\, 2k_B(T_p - T_g)$$

Conduction
Nanoparticles cool as surrounding gas atoms scatter from surface. This includes the unknown accommodation coefficient, α.

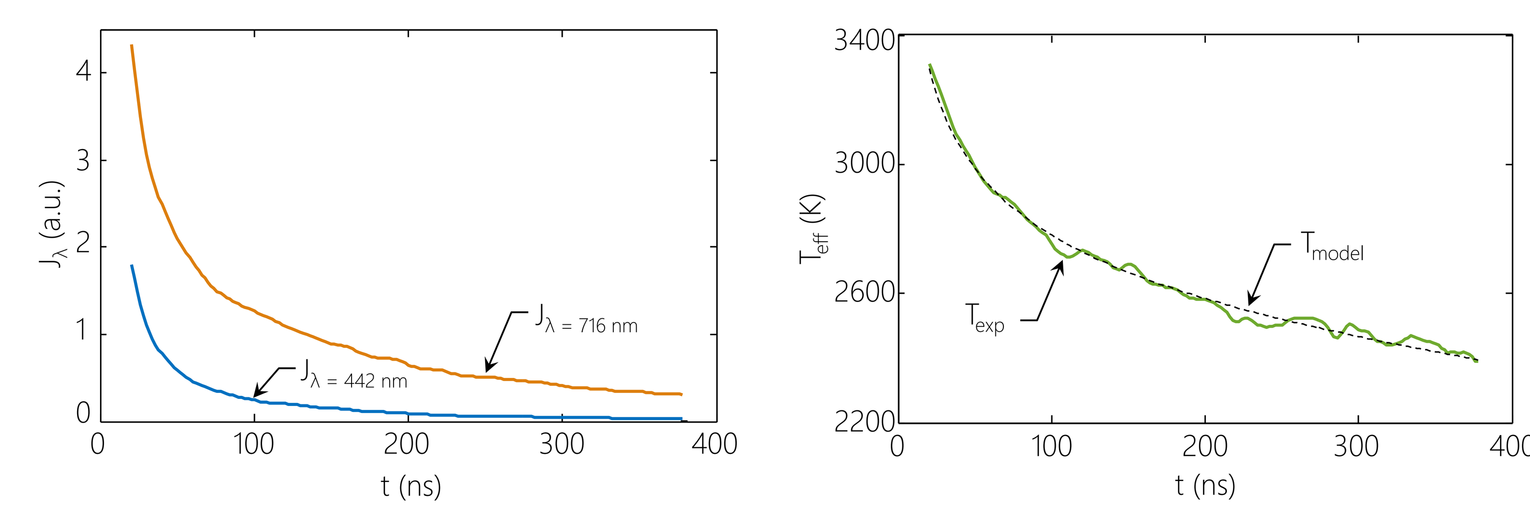

The above graphs show (left) the incandescence collected for Fe-Ar and (right) the experimental and modelled pyrometric effective temperature decay from those signals.

MOLECULAR DYNAMICS

The accommodation coefficient can be calculated by molecular dynamics [3].

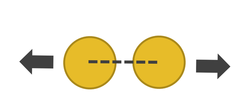

Embedded Atom Model
Models interaction between Fe-Fe atoms; contains pairwise repulsive and many-body attractive components.

$$U_i(r_{ij}) = F_\alpha \sum_{i\neq j} \rho_\beta(r_{ij}) + \frac{1}{2}\sum_{i\neq j} \phi_{\alpha\beta}(r_{ij})$$

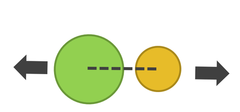

Morse Potential
Fe-He and Fe-Ar potentials are parameterized by fitting the sum of pairwise Morse potentials to ground state energies derived using density functional theory.

$$U_{ij} = D_M\left[1 - e^{-\alpha(r-R)}\right]^2$$

The nanoparticle surface is brought to 2400 K using a Nosé-Hoover thermostat. Incident gas molecular velocities are sampled from a Maxwell-Boltzmann distribution at 300 K. The thermal accommodation coefficient is found by comparing the kinetic energy of incident and scattered gas molecules.

$$\alpha = \frac{(1/2)m_g\left\langle v_{g,o}^2 - v_{g,i}^2 \right\rangle}{2k_B(T_p - T_g)}$$

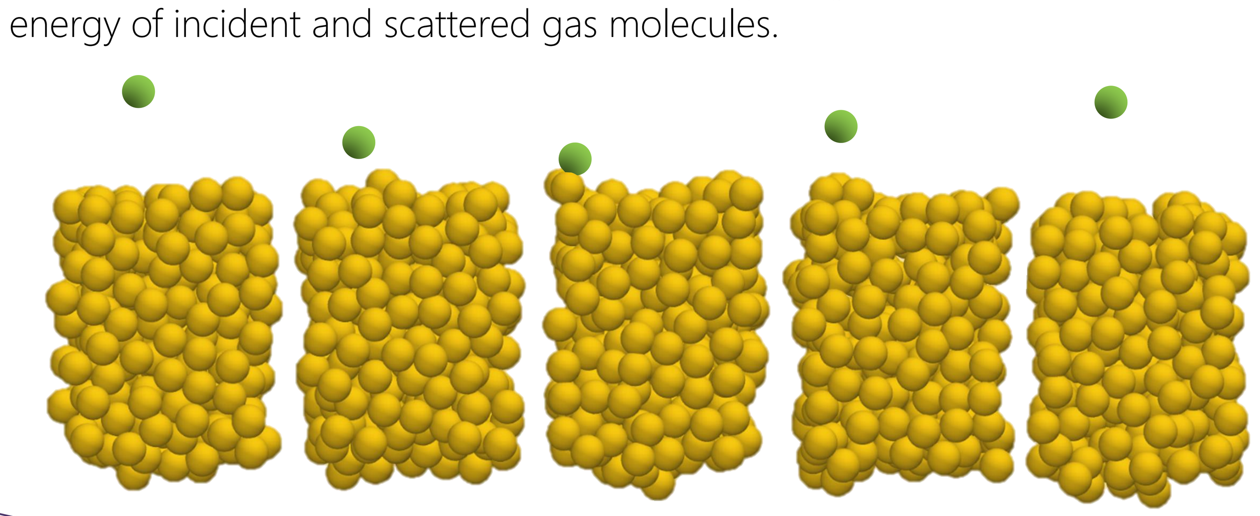

RESULTS

The following table contains the inferred parameters from the present study and previous parameters from comparable work:

Gas-Surface Pair	d_p [nm]	α			
		Present study (Exp.)	Daun et al. (MD) [3]	Eremin et al. (Exp.) [4]	Kock et al. (Exp.) [5]
Fe-He	53 ±13	0.06 ±0.05	0.11 ±0.01	0.01	-
Fe-Ar	39 ±6	0.17 ±0.08	0.23 ±0.03	0.1	0.13
Fe-N_2	42 ±8	0.17 ±0.07	-	-	0.13
Fe-CO_2	45 ±11	0.28 ±0.14	-	-	-

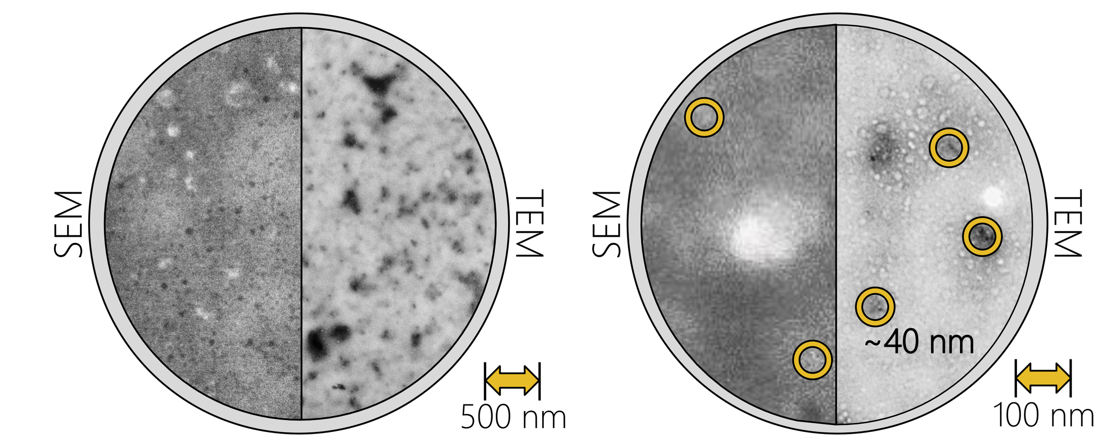

Electron Microscopy
Image fuzziness is suspected to be due to the stabilizing polymer that prevents monomer agglomeration.

Size Comparison (Fe-Ar)
Nanoparticle sizes are generally consistent. TiRe-LII sizes should be slightly smaller because of the lack of oxidation and polymer cap.

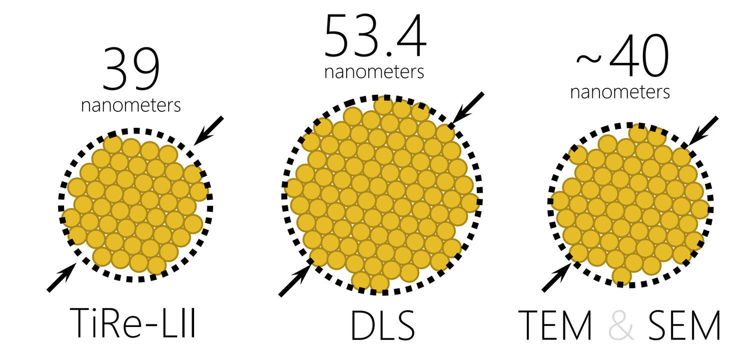

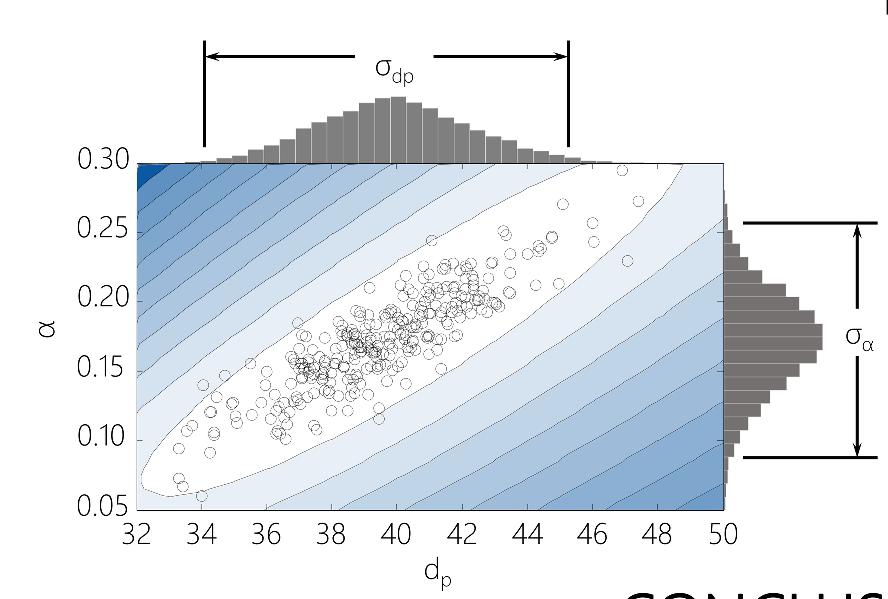

Robust Bayesian Analysis
The underlying ill-posedness of the problem amplifies measurement noise (mainly photomultiplier shot noise) into large credibility intervals. These intervals are represented in the error bounds presented in the table above.

CONCLUSIONS

1. The accommodation coefficient inferred in the present work is: (i) smaller than those found by molecular dynamics, (ii) consistent with previous experiments, and (iii) accompanied by fairly large error bounds.
2. The particle size is relatively consistent across the measurement techniques with TiRe-LII being the smallest, likely due to the removed polymer can and lack of oxidation.

FUTURE WORK

1. Apply robust Bayesian analysis to measurement data from Kock et al. [5] to retrieve nanoparticle sizes and accommodation coefficients.
2. Continue work with molecular dynamics to resolve discrepancies and calculate the accommodation coefficient for the polyatomic gas molecules.

REFERENCES

[1] D. L. Huber et al., (2005). *Small.* **1**, pp. 482-501.
[2] Y. Liu et al. (2005). *Env. Sci Technol.* **39**, pp. 1338-1345.
[3] K. J. Daun et al. (2013). *Appl. Phys. B.* **112**, pp. 599-600.
[4] A. Eremin, et al. (2008) *J. Phys. D.* **41**, 055203.
[5] B. F. Kock, et al. (2005). *Proc. Combust. Inst.* **30**, pp. 1689-1697.

ACKNOWLEDGEMENTS

NSERC CRSNG
Waterloo Institute for Nanotechnology